Suusamyr, Kyrgyzstan
Structural-geological Report

by David Fossati
fossatid@student.ethz.ch

Contents

1 Introduction

In September 2007 I spent 18 days in the area of Suusamyr Valley doing structural-geological field work. The goal of the field work was to determine the direction and sense of shear of fault displacements. This informations should contribute to the realization of the geological map of the region.

2 Field work area

The field work region was in the area of the Suusamyr Valley, SW of Bishkek, the capital of Kyrgyzstan (see figures 1 and 2). This zone lies in the Tien Shan mountain range, a part of the Himalayan orogenic belt which was formed by the collision of the Indian and Eurasian plates in the Cenozoic era. The analysed region can be subdivided in the following areas:

- Töö-Ashuu Pass Region
- E of Taldy-Bulak
- Ala-Bel Pass Region
- SE of Ötmök
- Karakol Pass

Topographic maps

The used topographic maps 1:100’000 which were produced 1990 by the ‘Kyrgyz Social Soviet Republic’ SSR are (see figure 3):

- K-43-39
- K-43-40
- K-43-41
- K-43-42
- K-43-63
- K-43-64
- K-43-65
- K-43-66

Figure 1: Geografical overview of Kyrgyzstan (image from: http://geology.com/world/kyrgyzstan-satellite-image.shtml)

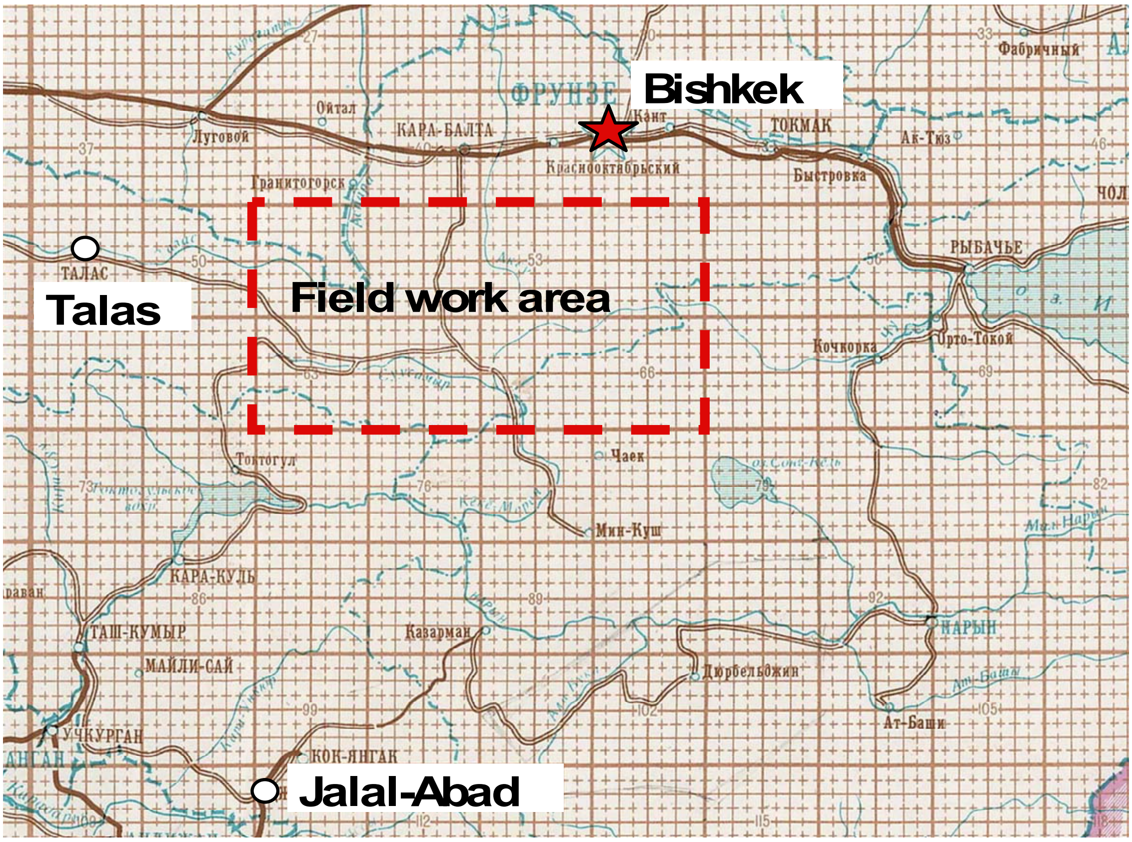

Figure 2: Field work area

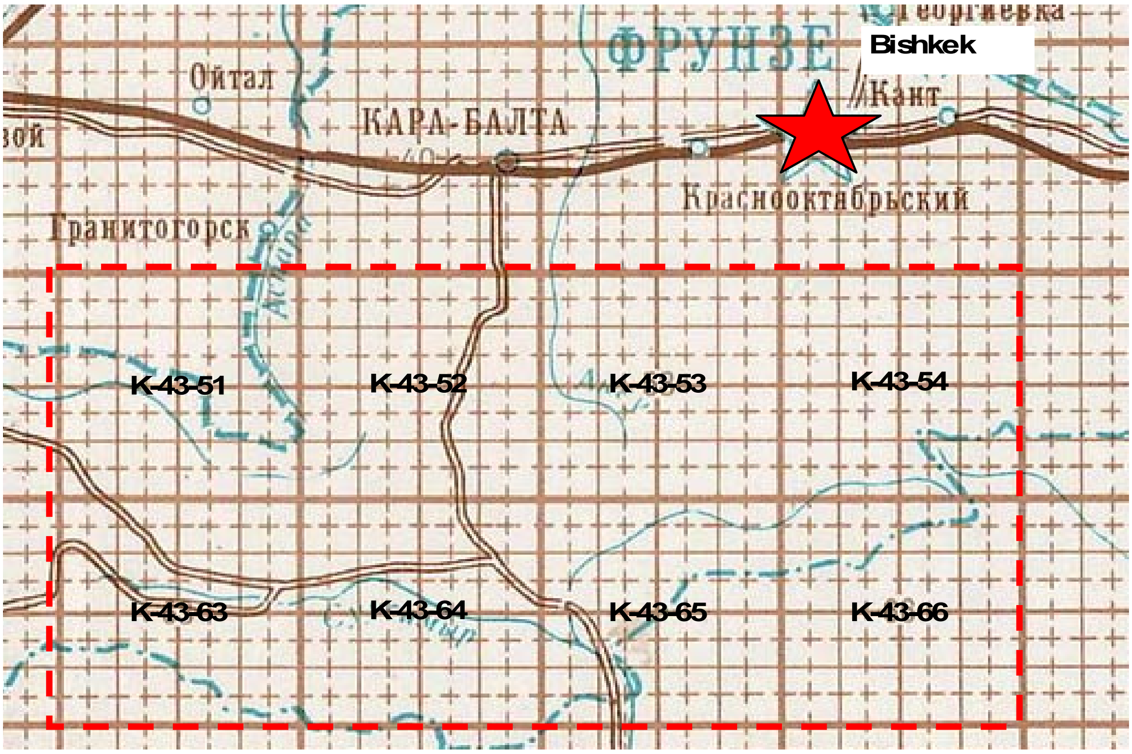

Figure 3: Topographic map location of the field area

3 Field work methods

To determine the direction and the sense of movement of the fault displacements I searched appropriate outcrops along the already mapped fault areas. The most difficult part of the work was to find good outcrops. These are unfortunately very rare. The direction and the sense of movement could be determined from striations, slickensides and half-moon structures.

Striations are mostly produced by minerals fibres in fine material along the fault plane. Some striations can also be produced by hard objects driven along the fault surface. The striations give an information about the direction of the movement.

Slickensides are parallel striations on rock surfaces often composed of fibrous crystals that stretch from one side of the fault plane to the other. These are produced by relative motion between opposite sides of fault planes and are commonly associated with brittle faulting [McClay, 1987]. Slickensides form by the progressive crystallization of minerals on the fault surface as the fault slips. When the fault has little steps or irregularities, sliding produces space in which minerals can crystallize. Typical precipitation minerals are calcite, quartz and chlorite. The fibers build on the fault surface steps and can be used to determine the sense of movement. The surface with the fibres moved from the step in the direction where fibres are going.
From slickensides outcrops I collected the following data:

- the orientation of the fault surface and the plunge of lineation
- observations about fault rock, sense of movement from fibers and steps in the fault plane and the nature of fiber growth

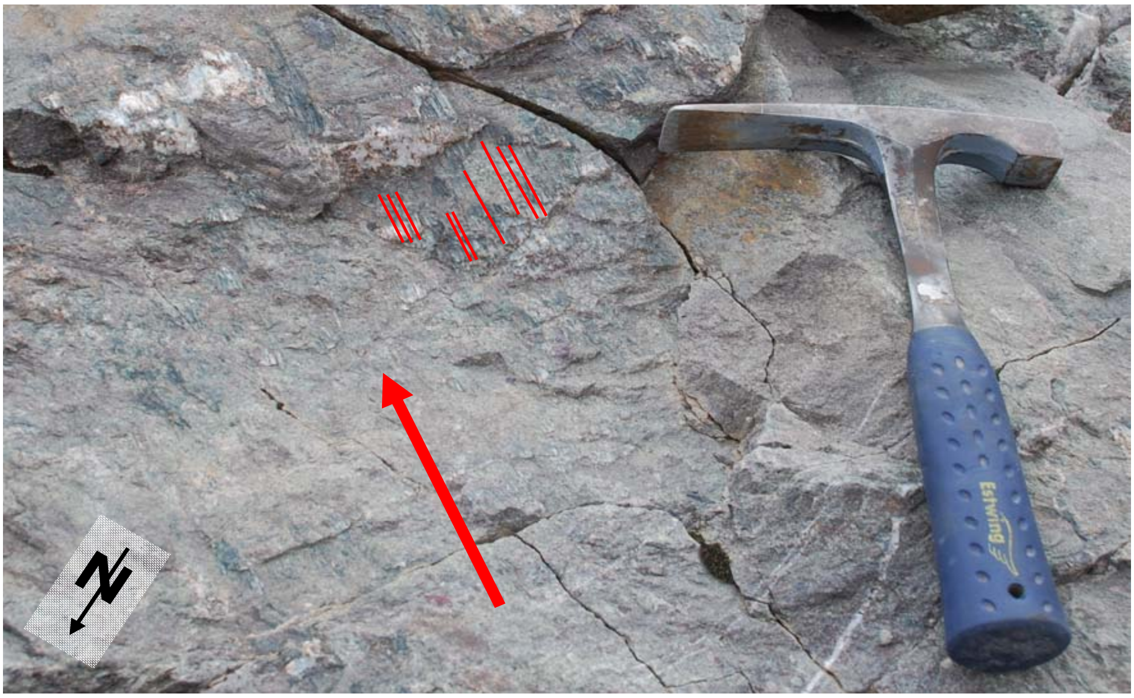

Picture 1: Slickensides example from Karakol Pass

Half-moon structures are structures derived from objects which were pressed and driven along a surface. This moving objects leave a mark on the rock in the direction of movement. By half-moon structures the leading edges show the direction of the removed block.

From half-moon structures I collected the following data:

- measured the orientation of the fault surface and the plunge of the leading edges
- record observations about fault rock and the sense of movement from the leading edges

Picture 2: Half-moon structure example from SW Töö-Ashuu Pass

GPS measurements, when possible, were collected in all interesting outcrops. The others coordinates hat to be deducted from the map.

4 Analysis methods

The goal of the slickensides and half-moon structure measurements is the evaluation of the orientation of the paleostress tensors. This means the orientation of the principal axes of the stress ellipsoid at the time of faulting.

The evaluation of the paleostress is a statistical computation. This means that the value is an approximation for the faults in a geological significant time and is not a true paleostress tensor. In this sense the term stress is not appropriate because the result is not related to an instantaneous information at one point. However this information is an approximation of the forces which were responsible for the brittle deformation [Burg, 2006].

To evaluate the paleostress tensors we used the Programm FSA 28.3 of Célérier. This program analyses fault and stress tensor data. The input data must include the dip and orientation of the fault plane and the sense and the direction of movement of the faults measured on slickensides or on half-moon structures. The Program uses random stress tensors to evaluate the best tensor for the fault and dip data. The best analytical solutions can then be graphically visualized, which then allows to choose the best solution.

The output sheets show 4 graphics. The graphic in the upper left corner displays all measurements. The graphic in the upper right corner shows the 3 main stresses in form of a pentagon (σ1), a square (σ 2) and a triangle (σ 3). The graphic in the centre shows the measured points in a Mohr diagram. To be consistent the measurements must lie between the old failure criteria (the line going through the origin) and the new failure criteria (the upper line). The graph at the bottom shows the angles between the measured bedding and the evaluated stress tensor. This angle should not exceed 30° to correspond to the main stress σ1. This means that relevant measurements must lie between 0°-30° and 150°-180°, while the others do not correspond to the main stress [Ghirardello, 2006].

5 Maps and analysis results

Töö-Ashuu Pass Region

In this region 4 areas along faults were investigated. The results are shown in the figures 4 & 5. The field data and the evaluated data with the FSA program are given in the appendix.

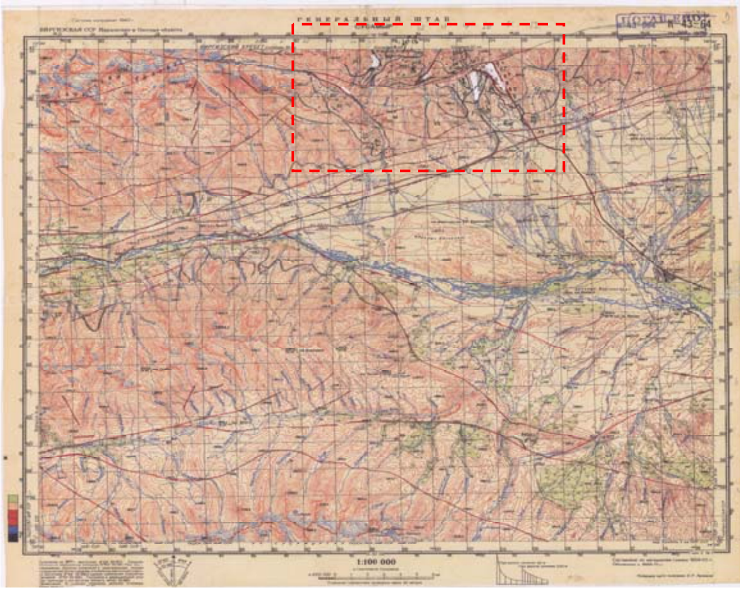

Figure 4: Map K-43-64

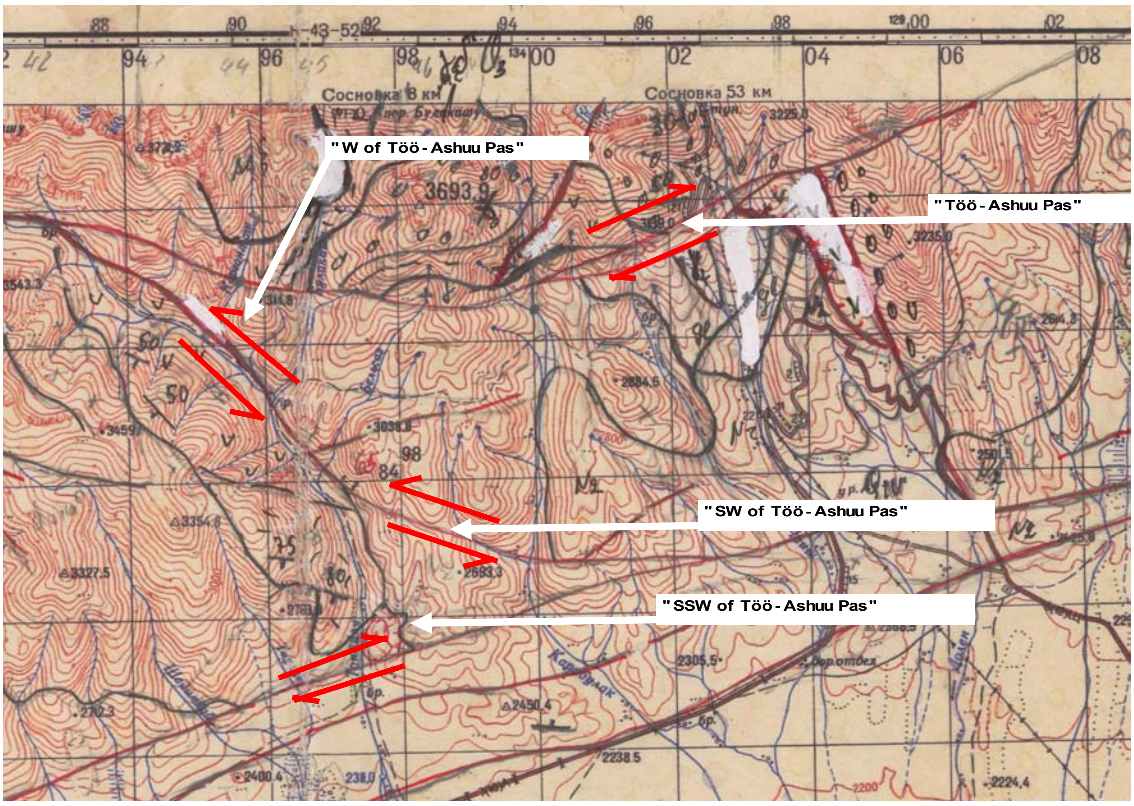

Figure 5: Part of the map K-43-64 with the faults and the displacement directions

E of Taldy Bulak

In this region 1 fault was investigated. The results are shown in the figure 6 & 7. The field data and the evaluated data with the FSA program are given in the appendix.

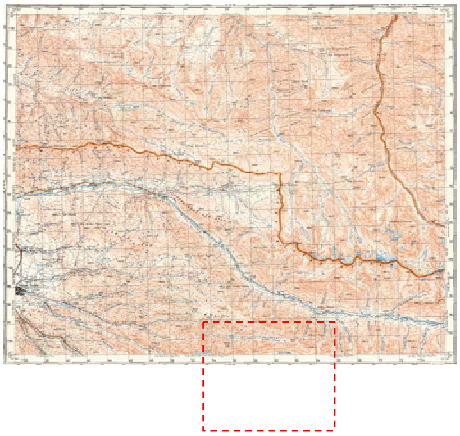

Figure 6: Maps K-43-51 and K-43-63

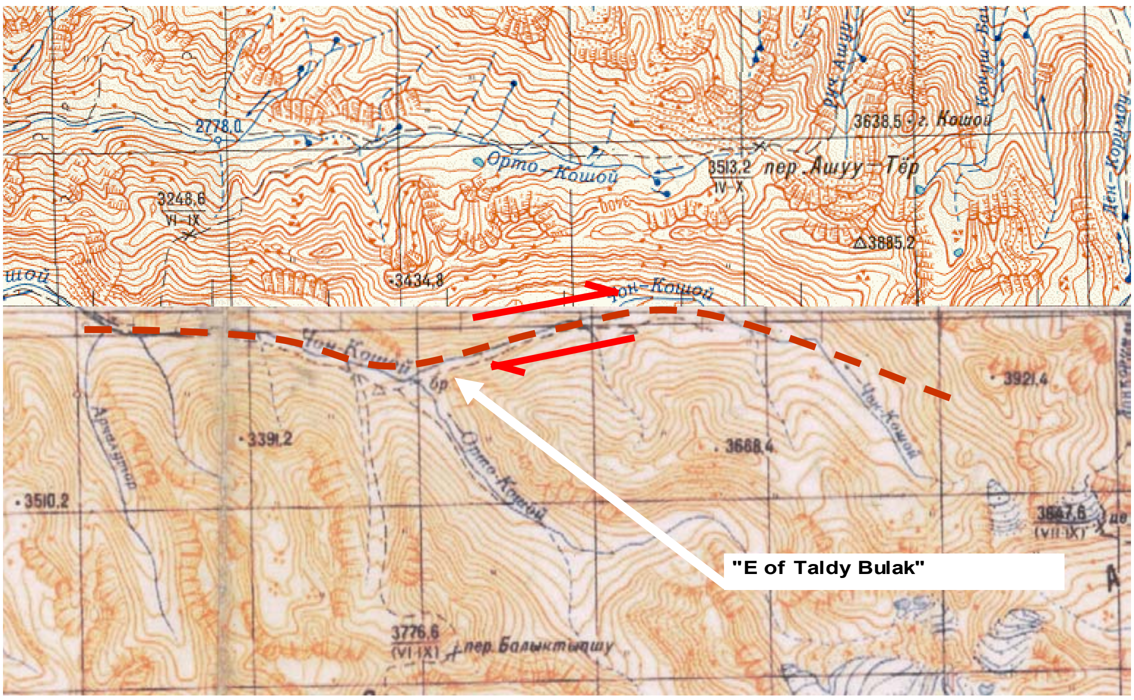

Figure 7: Part of the maps K-43-51 and K-43-63 with the faults and the displacement directions

Ala-Bel Pass Region

In this region 1 fault system was investigated. The results are shown in the figures 8 & 9. The field data and the evaluated data with the FSA program are given in the appendix.

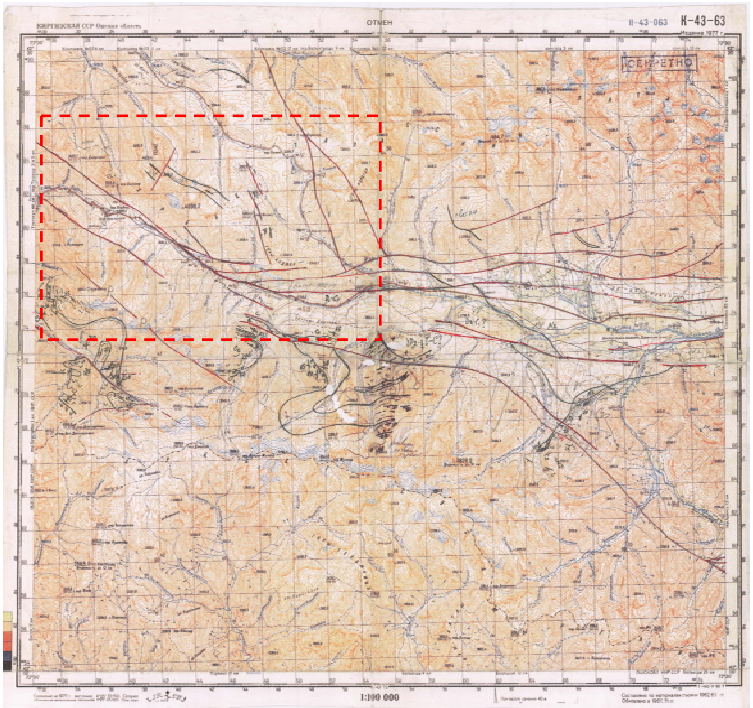

Figure 8: Map K-43-63

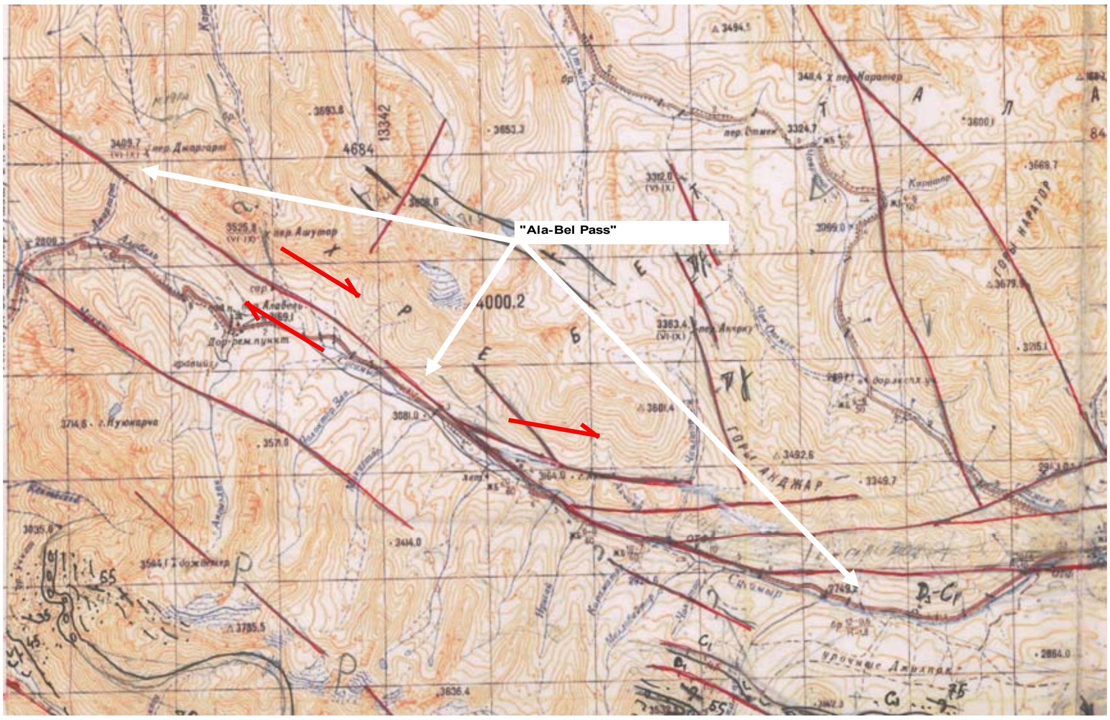

Figure 9: Part of the map K-43-63 with the faults and the displacement directions

SE of Ötmök

In this region 1 fault system was investigated. The results are shown in the figures 10 & 11. The field data and the evaluated data with the FSA program are given in the appendix.

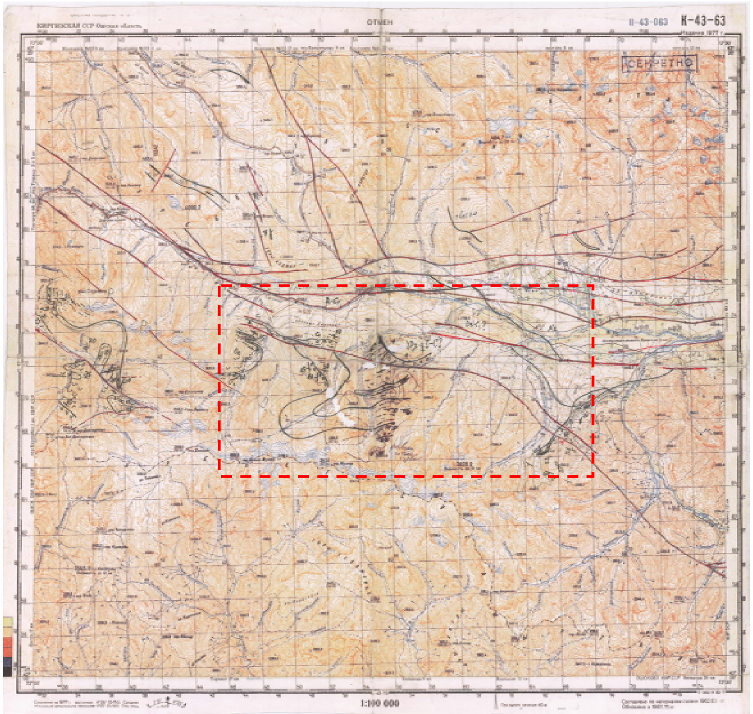

Figure 10: Map K-43-63

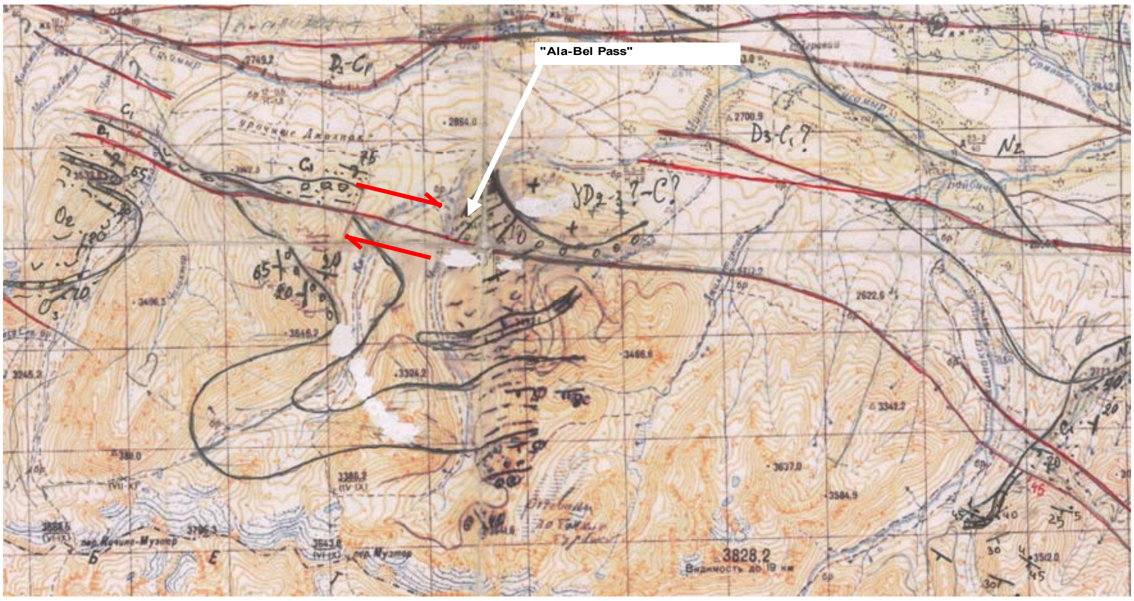

Figure 11: Part of the map K-43-63 with the faults and the displacement directions

Karakol Pass

In this region 2 fault systems were investigated. The results are shown in the figure 12 & 13. The field data and the evaluated data with the FSA program are given in the appendix.

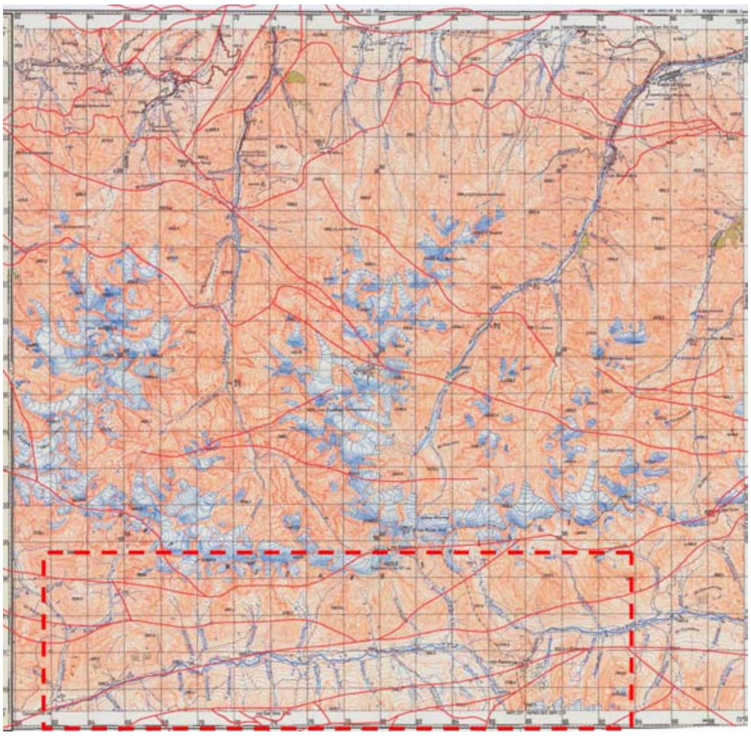

Figure 12: Map K-43-54

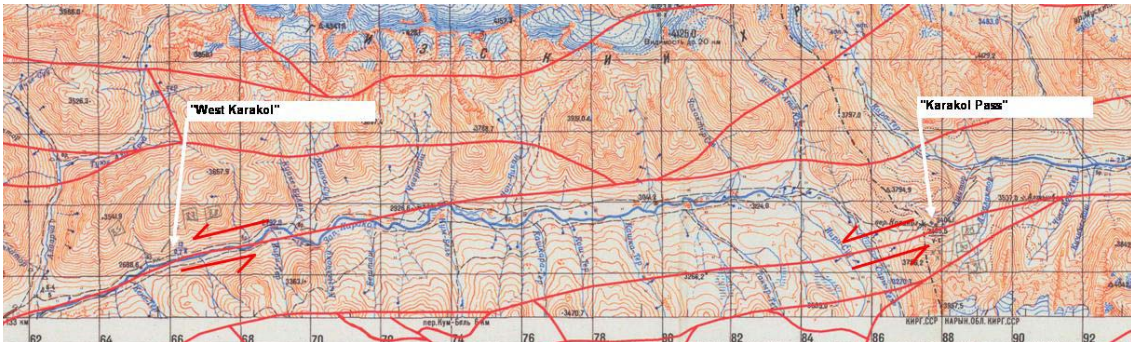

Figure 13: Part of the map K-43-54 with the faults and the displacement directions

6 References and Literature

Bons, P. Structural Geology Skript. Eberhard Karls Universität Tübingen.

Burg, J.P. 2004. Vorlesungsskript Grundzüge. ETH Zürich.

Burg, J.P. 2006. Vorlesungsskript Tektonik. Referenced in: Ghirardello, B. 2006. Visuelle Satellitenbildanalyse rezenter geomorphologischer Strukturen im Thien Shan, Kyrgyzstan. Diplomarbeit. Geologisches Institut Universität Zürich.

Ghirardello, B. 2006. Visuelle Satellitenbildanalyse rezenter geomorphologischer Strukturen im Thien Shan, Kyrgyzstan. Diplomarbeit. Geologisches Institut Universität Zürich.

McClay, K. R. 1987. The mapping of geological structures. Geological Society of London. Handbook Series.

7 Appendix: Field data and analysis graphs

Töö-Ashuu Pass Region

"Töö-Ashuu Pass, 19 September 2007"

Coordinates N [°]	E [°]	Strike	Dip	Dip direction	Slickenside	Muvement type*	Fault Number	Foto Number
42.31675	73.81259	35	75	'E'	49	'N'	28	401/402
42.31675	73.81259	76	30	'E'	125	'D'	29	
42.31675	73.81259	45	39	'E'	75	'D'	30	
42.31675	73.81259	90	34	'N'	286	'S'	31	
42.31675	73.81259	50	30	'E'	170	'S'	30	403

* [D=Dextral; S=Sinistral; N=Normal; I=Inverse]

"Suusamyr valley W Töö-Ashuu Pass, 8 September 2007"

Coordinates N [°]	E [°]	Strike	Dip	Dip direction	Slickenside	Muvement type*	Fault Number	Foto Number
42.30513	73.72448	5	57	'E'	7	'S'	1	121
42.30513	73.72448	140	62	'N'	135	'S'	1	122
42.30786	73.72361	70	70	'W'	268	'D'	2	131
42.30778	73.72320	49	65	'W'	232	'S'	3	132
42.30525	73.72931	31	86	'E'	30	'N'	4	134

* [D=Dextral; S=Sinistral; N=Normal; I=Inverse]

"Suusamyr valley SW Töö-Ashuu Pass, 9 September 2007"

Coordinates N [°]	E [°]	Strike	Dip	Dip direction	Slickenside	Muvement type*	Fault Number	Foto Number
42.27860	73.76704	150	85	'S'	138	'I'	5	150
42.27860	73.76704	152	80	'S'	160	'D'	5	151
42.27860	73.76704	140	82	'S'	155	'I'	5	152
42.27860	73.76704	138	82	'S'	137	'I'	5	

* [D=Dextral; S=Sinistral; N=Normal; I=Inverse]

"Suusamyr valley SSW Töö-Ashuu Pass, 19 September 2007"

Coordinates N [°]	E [°]	Strike	Dip	Dip direction	Slickenside	Muvement type*	Fault Number	Foto Number
42.26439	73.75881	98	62	'S'	117	'N'	26	397
42.26724	73.75790	47	85	'W'	240	'N'	27	398
42.26724	73.75790	46	84	'W'	235	'N'	27	399
42.26724	73.75790	53	69	'W'	246	'N'	27	
42.26724	73.75790	46	63	'W'	240	'N'	27	

* [D=Dextral; S=Sinistral; N=Normal; I=Inverse]

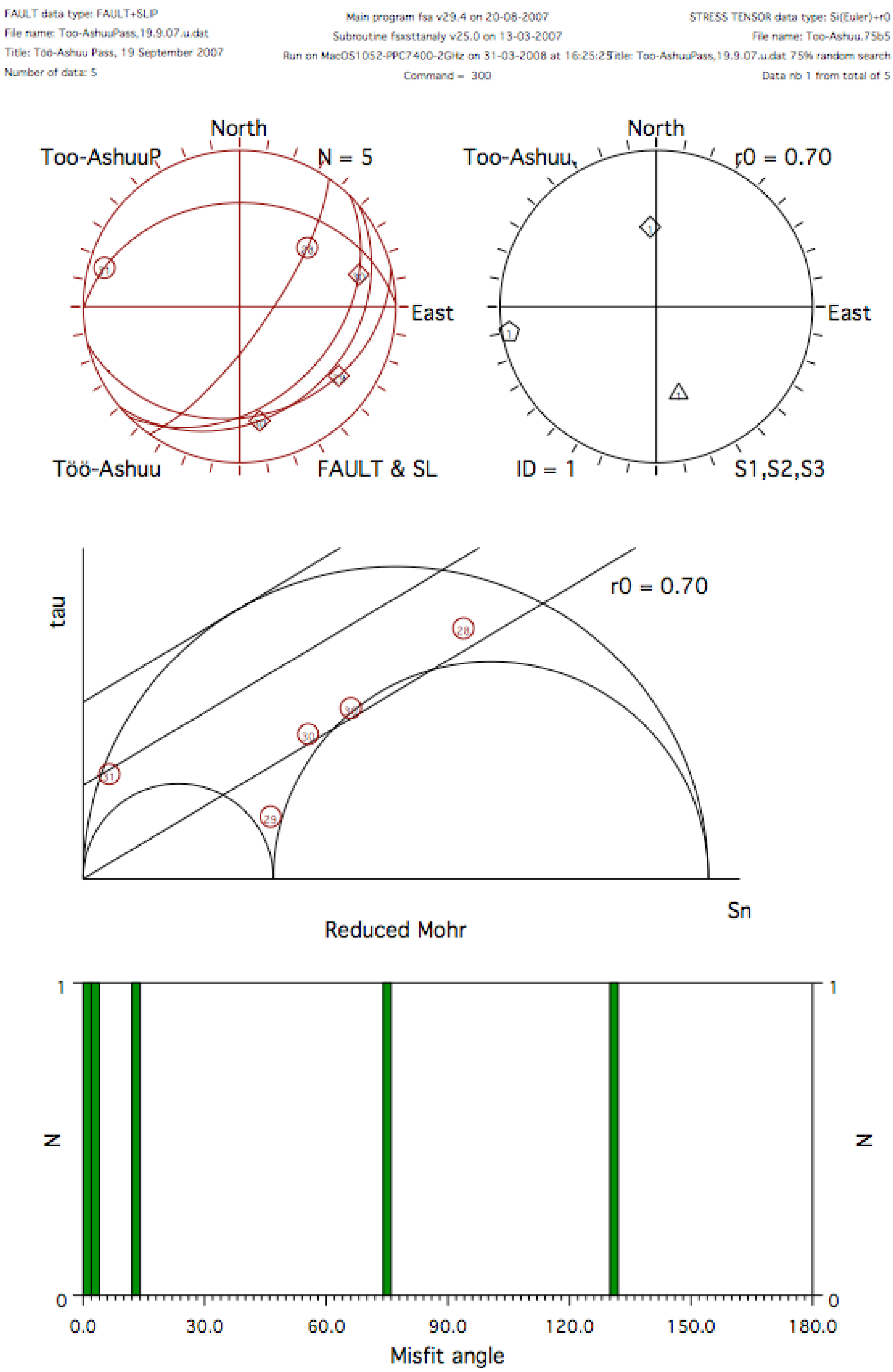

Figure 14: Paleostress tensor graphs of “Töö-Ashuu Pass”

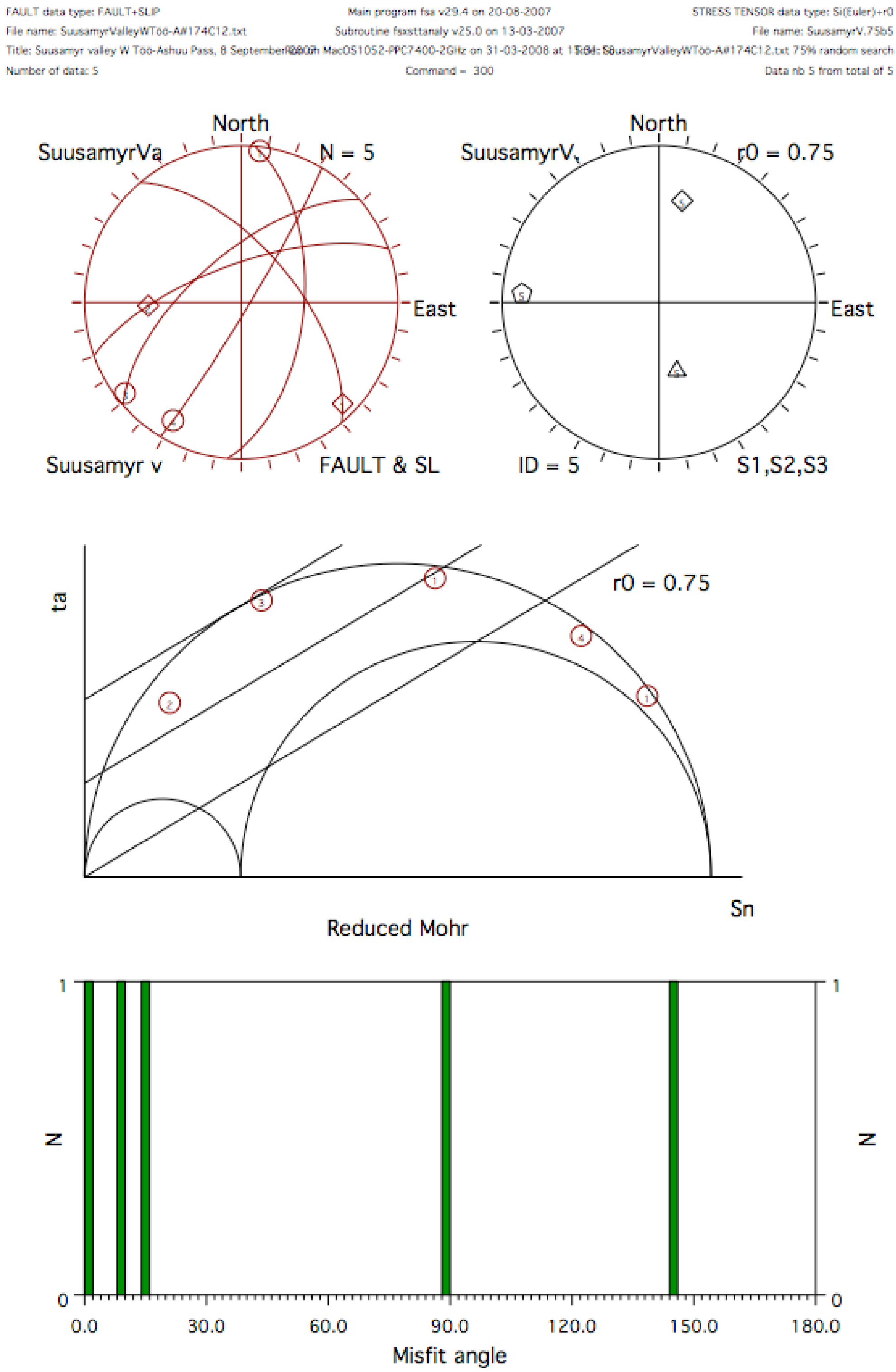

Figure 15: Paleostress tensor graphs of "Suusamyr valley W Töö-Ashuu Pass"

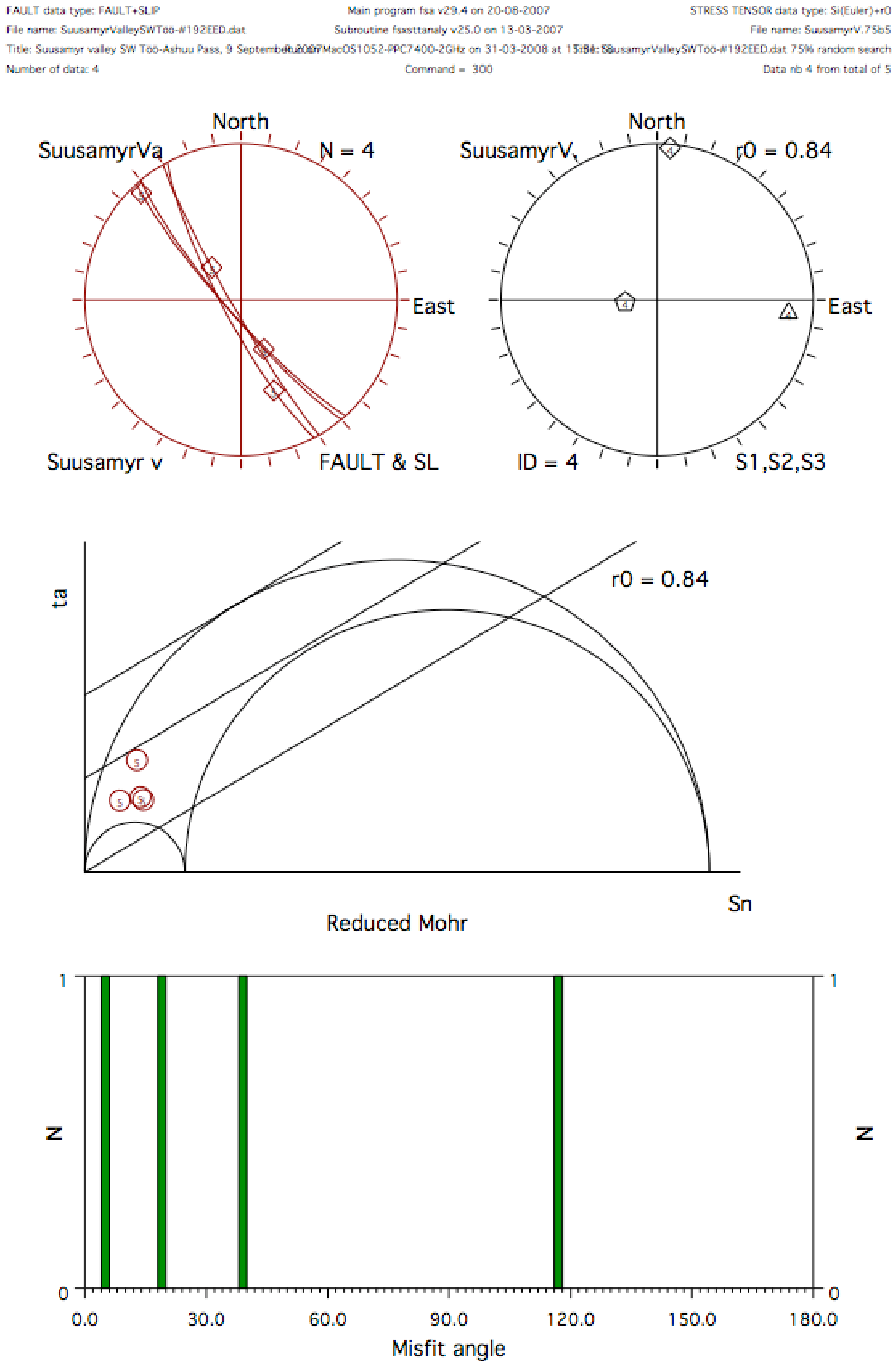

Figure 16: Paleostress tensor graphs of "Suusamyr valley SW Töö-Ashuu Pass"

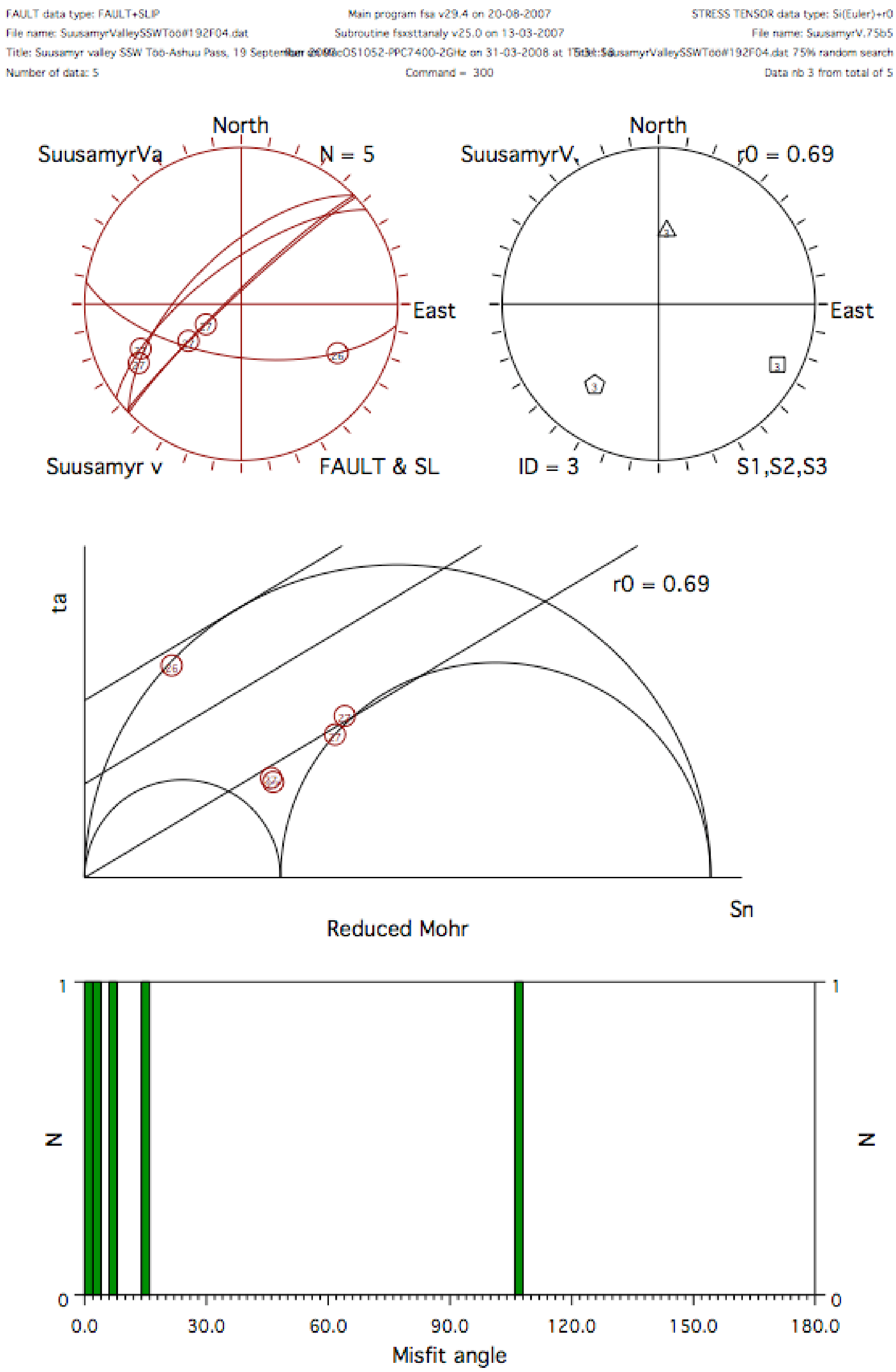

Figure 17: Paleostress tensor graphs of "Suusamyr valley SSW Töö-Ashuu Pass"

E of Taldy Bulak

"E of Taldy-Bulak, 15 September 2007"

Coordinates** N [°]	E [°]	Strike	Dip	Dip direction	Slickenside	Muvement type*	Fault Number	Foto Number
42.32778	73.30000	52	85	'E'	222	'D'	9	291
42.32778	73.30000	91	78	'N'	85	'D'	10	293
42.32778	73.30000	92	82	'N'	91	'N'	10	294
42.32778	73.30000	88	80	'W'	79	'N'	10	295
42.32778	73.30000	110	83	'N'	81	'N'	11	296
42.32778	73.30000	105	78	'N'	82	'N'	11	
42.32778	73.30000	88	80	'E'	95	'D'	12	300
42.32778	73.30000	108	68	'N'	100	'D'	13	
42.32778	73.30000	109	72	'N'	110	'D'	13	
42.32778	73.30000	60	80	'E'	68	'I'	14	301
42.32778	73.30000	101	89	'S'	96	'D'	15	

* [D=Dextral; S=Sinistral; N=Normal; I=Inverse]
** The coordinates are approximated

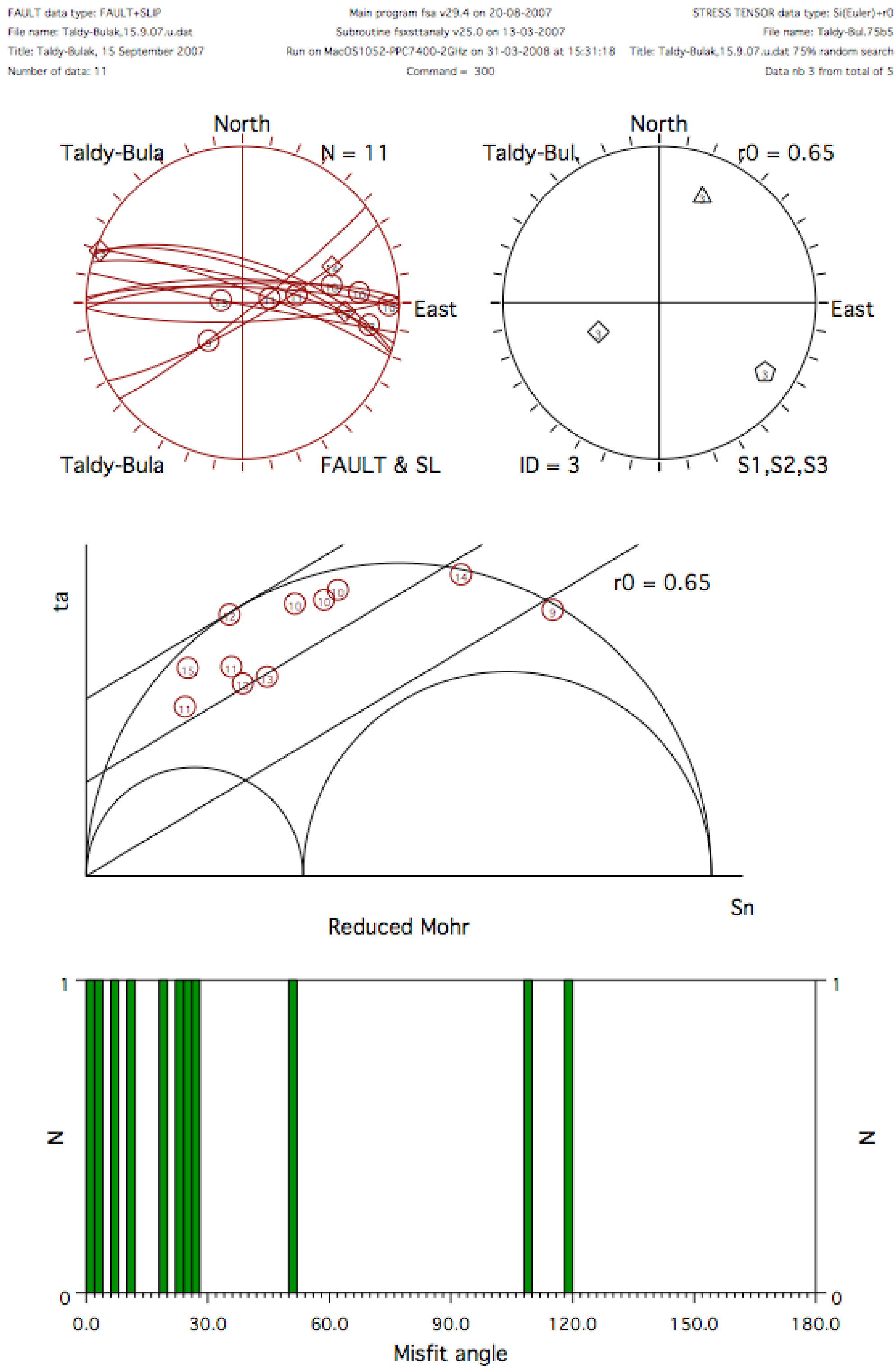

Figure 18: Paleostress tensor graphs of “E of Taldy Bulak”

Ala-Bel Pass Region

"Ala-Bel Pass, 16/17 September 2007"

Coordinates** N [°]	E [°]	Strike	Dip	Dip direction	Slickenside	Muvement type*	Fault Number	Foto Number
42.26806	73.02778	155	49	'S'	144	'D'	16	323/324
42.26833	73.03056	165	65	'N'	145	'D'	17	
42.26833	73.03056	167	62	'N'	136	'D'	17	325
42.26833	73.03056	154	55	'N'	144	'D'	17	327
40.26444	73.03333	125	86	'S'	298	'I'	18	328
40.26444	73.03333	120	70	'S'	275	'I'	18	
40.26444	73.03333	115	70	'N'	90	'N'	18	329 above
40.26444	73.03333	113	75	'S'	310	'I'	18	329 below
42.25639	73.04861	105	70	'N'	95	'S'	19	331
42.25639	73.04861	112	55	'N'	70	'D'	19	
42.23861	73.08556	135	55	'S'	185	'D'	20	
42.23861	73.08556	118	60	'S'	150	'D'	20	
42.20521	73.23677	45	79	'E'	50	'D'	21	
42.20521	73.23677	142	65	'N'	318	'D'	22	
42.20521	73.23677	91	84	'S'	98	'I'	23	341
42.20933	73.14445	130	65	'N'	340	'I'	24	342
42.23860	73.08571	155	46	'S'	165	'S'	25	343

* [D=Dextral; S=Sinistral; N=Normal; I=Inverse]
** The coordinates are approximated

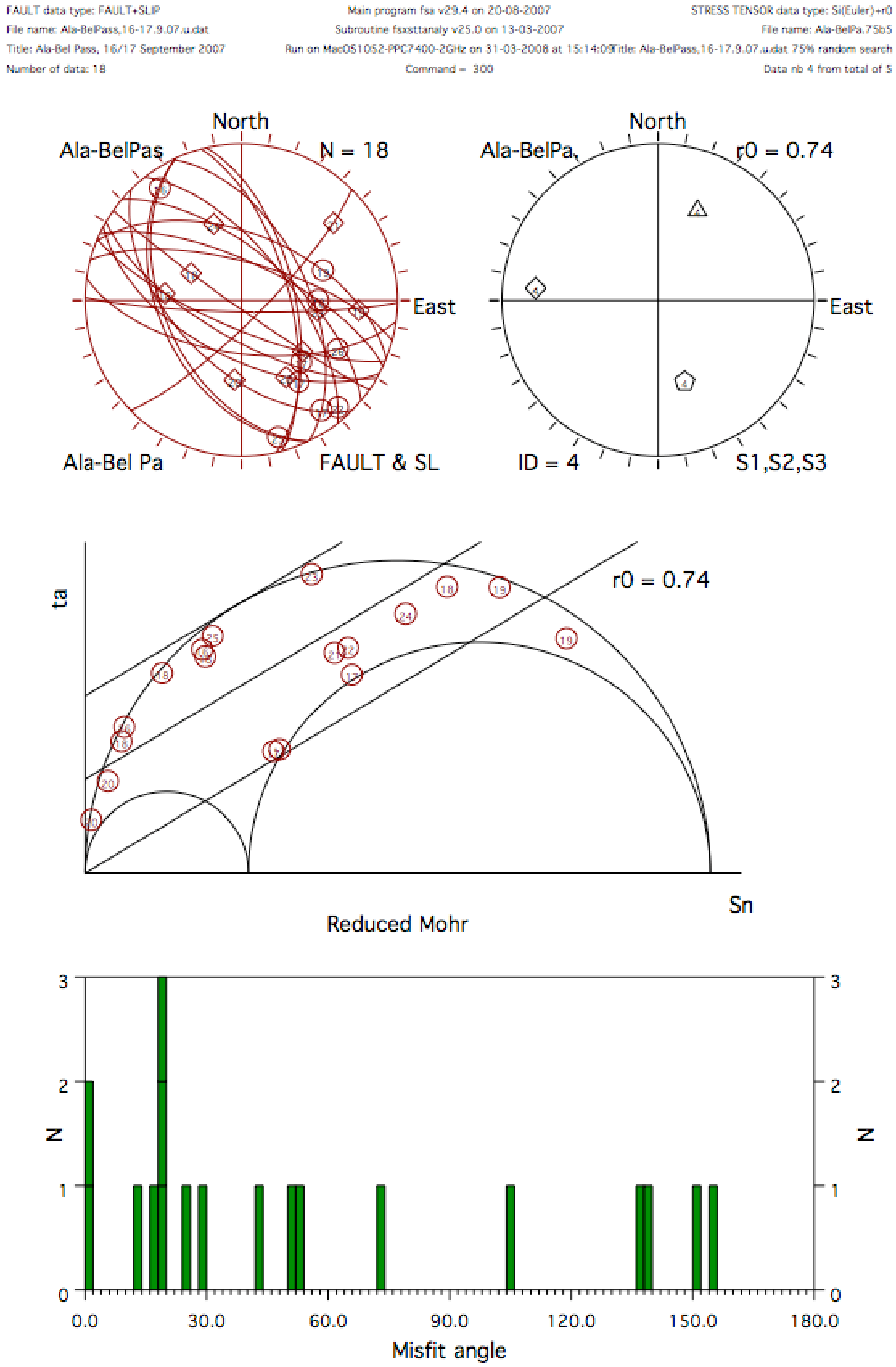

Figure 19: Paleostress tensor graphs of "Ala-Bel Pass Region"

SE of Ötmök

"Suusamyr valley SE Ötmök, 10 September 2007"

Coordinates N [°]	E [°]	Strike	Dip	Dip direction	Slickenside	Muvement type*	Fault Number	Foto Number
42.17372	73.24648	30	58	'W'	208	'S'	6	181
42.17372	73.24648	96	82	'S'	274	'D'	7	183
42.17372	73.24648	96	87	'S'	275	'D'	7	184
42.17041	73.24768	92	69	'S'	90	'D'	8	185
42.17041	73.24768	92	70	'S'	91	'D'	8	187

* [D=Dextral; S=Sinistral; N=Normal; I=Inverse]

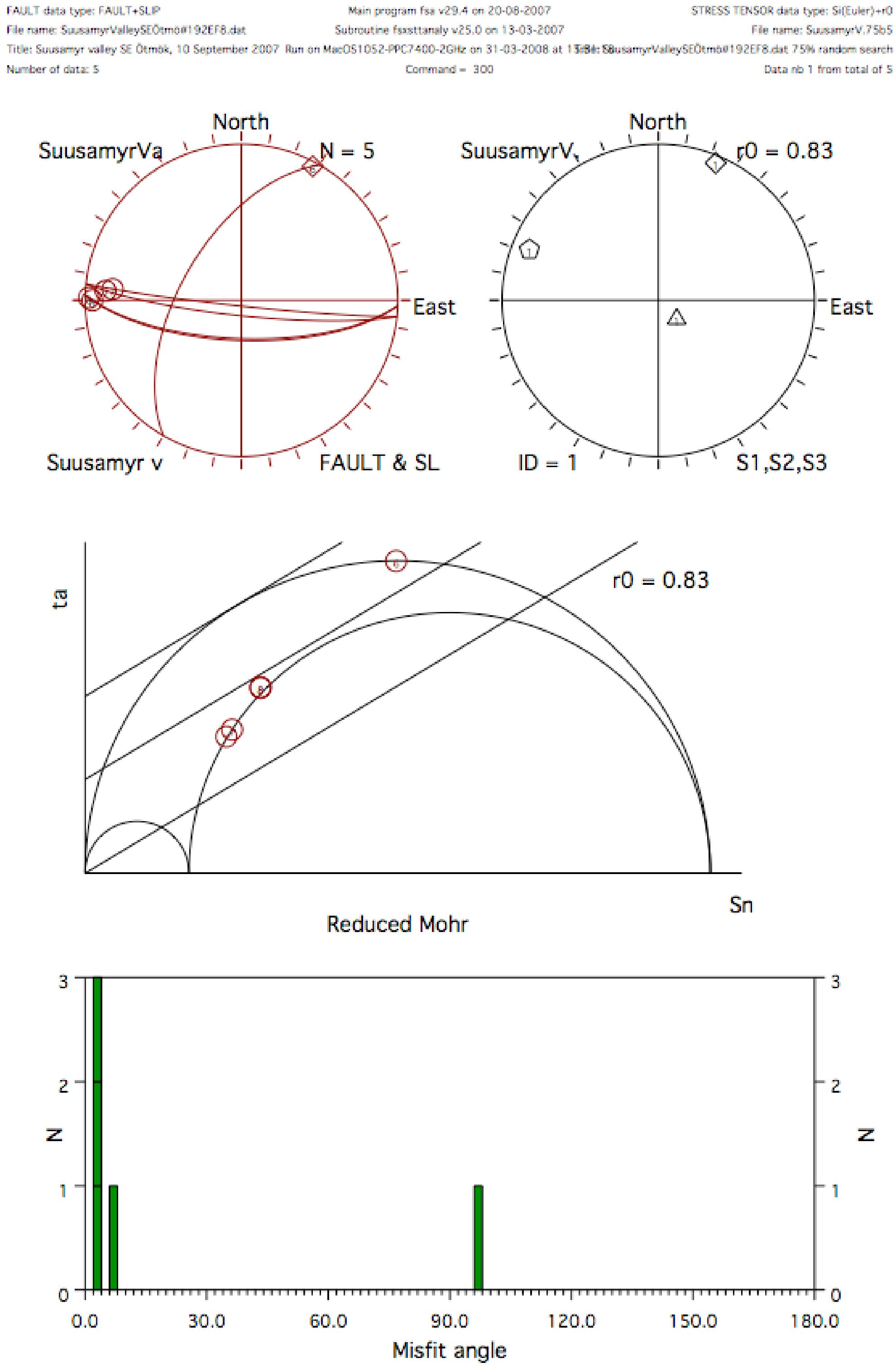

Figure 20: Paleostress tensor graphs of "SE of Ötmök"

Karakol Pass

"Karakol Pass, 20 September 2007"

Coordinates N [°]	E [°]	Strike	Dip	Dip direction	Slickenside	Muvement type*	Fault Number	Foto Number
42.34944	74.84812	91	63	'N'	107	'S'	35	420
42.34944	74.84942	49	23	'W'	40	'D'	36	421
42.34944	74.84942	21	50	'W'	259	'S'	37	424
42.34840	74.84936	91	56	'N'	309	'N'	35	425
42.34840	74.84936	63	46	'W'	300	'N'	38	426/427/428
42.34840	74.84936	61	49	'W'	331	'N'	38	

* [D=Dextral; S=Sinistral; N=Normal; I=Inverse]

"West Karakol, 20 September 2007"

Coordinates N [°]	E [°]	Strike	Dip	Dip direction	Slickenside	Muvement type*	Fault Number	Foto Number
42.34645	74.57741	176	84	'N'	169	'D'	32	412
42.34645	74.57741	166	84	'N'	154	'N'	32	
42.34713	74.58151	70	40	'W'	66	'S'	34	414/415

* [D=Dextral; S=Sinistral; N=Normal; I=Inverse]

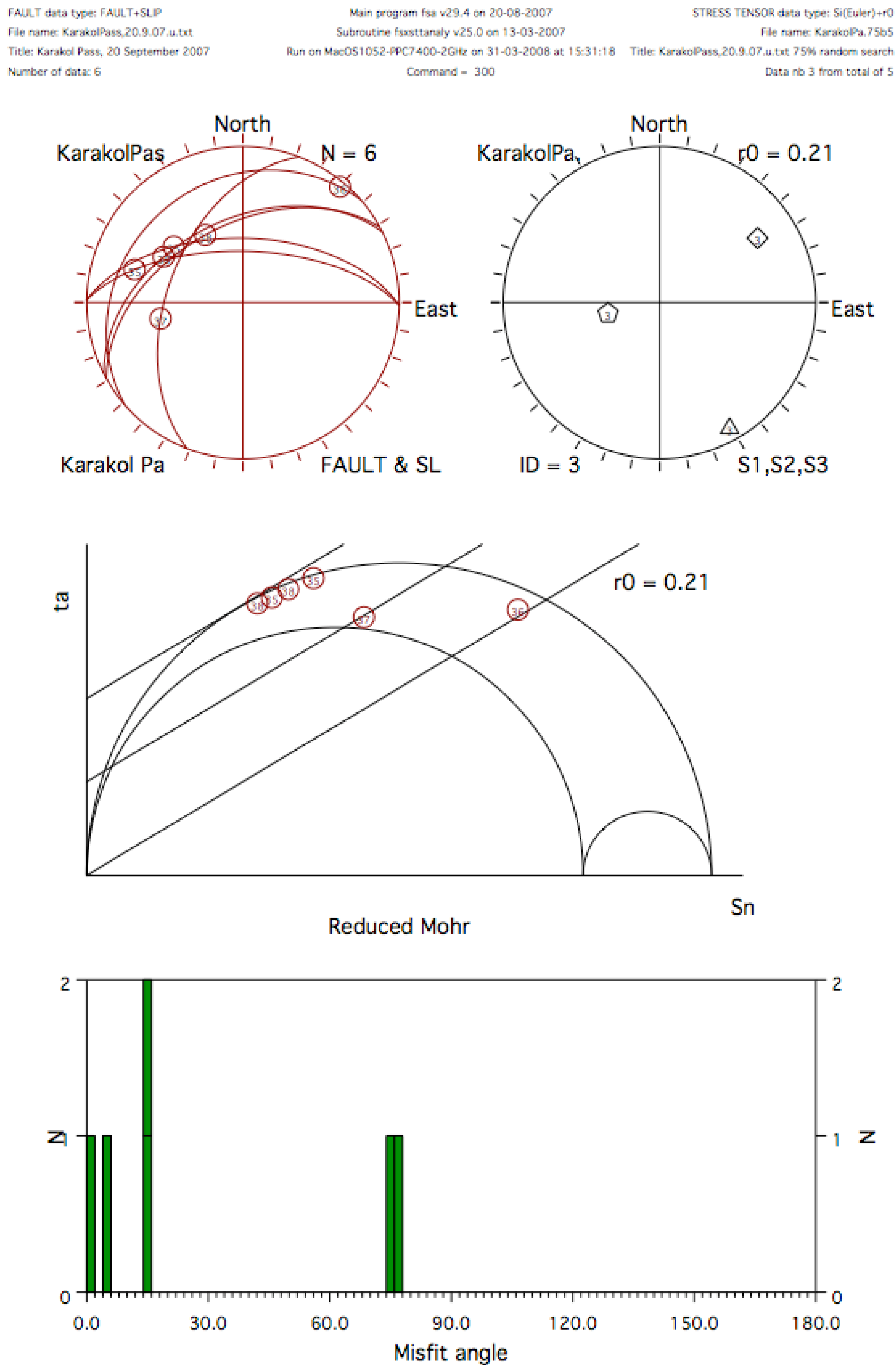

Figure 21: Paleostress tensor graphs of “Karakol Pass”

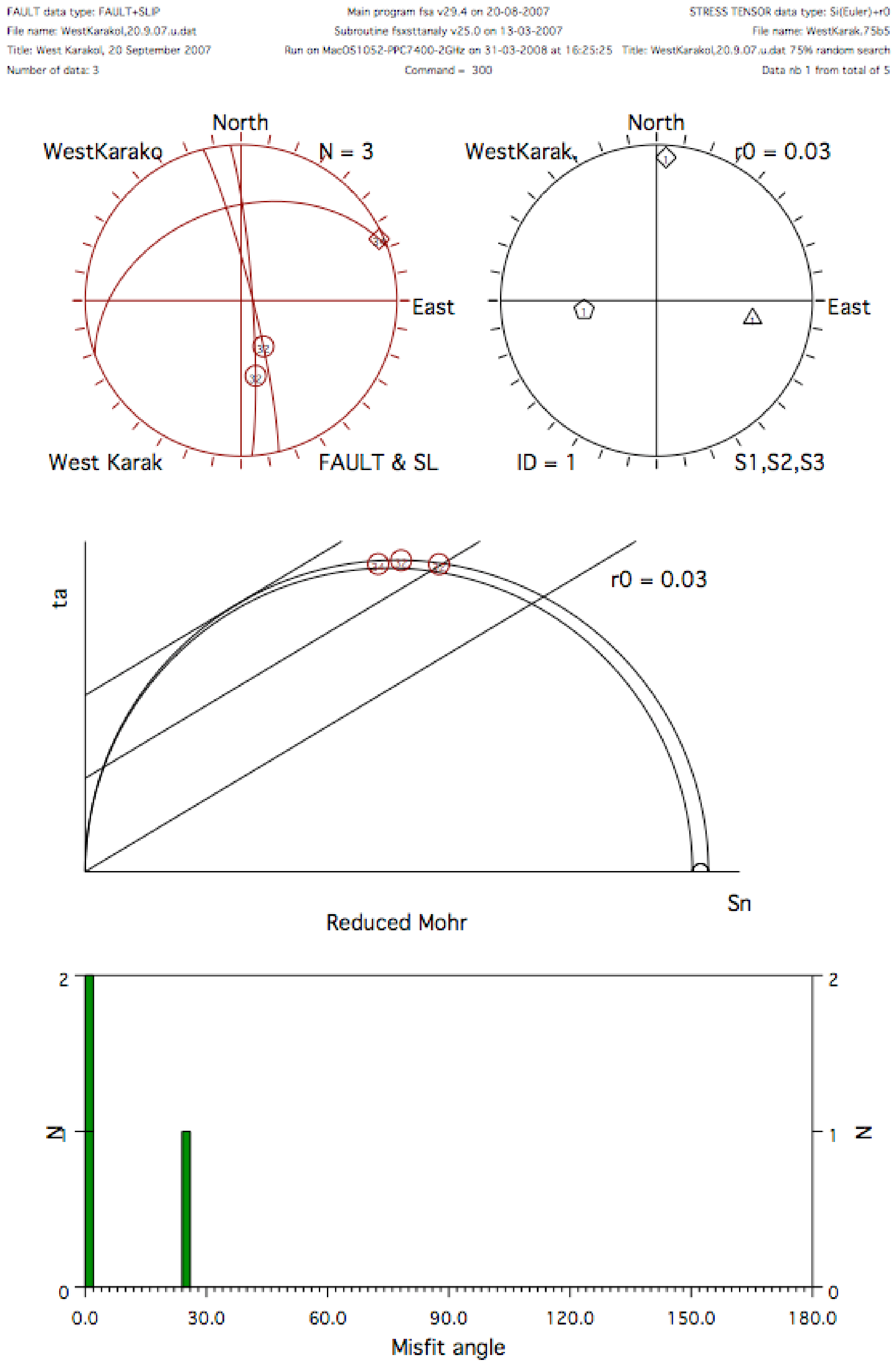

Figure 22: Paleostress tensor graphs of "West Karakol"